

Roles of Branch Content and Branch Length in Copolyethylene Crystallization: Molecular Dynamics Simulations

Xiu-bin Zhang, Ze-sheng Li,* Zhong-yuan Lu, and Chia-Chung Sun

Institute of Theoretical Chemistry, State Key Laboratory of Theoretical and Computational Chemistry, Jilin University, Changchun 130023, P. R. China

Received July 20, 2001; Revised Manuscript Received October 1, 2001

ABSTRACT: Molecular dynamics simulations of two series of single copolymer chain models with precisely controlled methyl branching and with branches of different lengths are performed. For the models with precisely controlled methyl branching, the collapse process and the morphology of the lamellar structure are similar to those of the random copolymer. In particular, it is found that the branch content plays an important role in determining whether a single chain can form a lamellar structure or not. With the decrease of the branch contents, more perfect lamellar structure is formed, and the crystallinity of the copolymer increases. For the models with branches of different lengths, the simulations show that the branch point (CH unit) is always expelled from the crystalline phase as a defect, while the behavior of the branch chain in the crystallization depends on the chain length. When the chain has less than 10 carbon atoms, the branch is rejected to the folded surface of the lamellar structure as a defect, whereas when the branch length is longer, the branch is folded back and cocrystallizes with the main chain. In this case, the branch chain is packed in a manner as in polyethylene.

I. Introduction

Linear low-density polyethylene (LLDPE) (copolymer of ethylene and an α -olefin) is a commercially important class of polyethylenes. Many experimental investigations^{1–16} have been performed to study the relationship between the microstructure and the crystal properties of the copolymer. It is known that the crystallizability is affected by molecular weight, concentration of branches, and their distribution along the copolymer backbone. To well understand the crystallization behavior of the branched molecules, the more homogeneous fractions of the copolymer are needed. However, the LLDPE samples normally have a heterogeneous microstructure, which makes it difficult to get experimentally more homogeneous fractions to systematically investigate the crystallization behavior of the branched molecules. Recently, ethylene copolymers with precisely controlled methyl branching have been created using acyclic diene metathesis (ADMET) chemistry as the mode of polymerization,^{17,18} which will provide the basis for a better understanding of the morphology, crystalline structure, and thermodynamics of the crystallization process of the copolymer. But to our knowledge, the information about the morphology and crystalline structure of the copolymer with well-controlled branching has not been reported yet.

Nowadays, the polymer models with well-controlled structures can be built easily by using simulation software, and the structural formation process of polymer chains can be investigated at the molecular level by means of the molecular dynamics (MD) simulation method. MD simulations^{19–22} starting from a single chain model have given us an insight into the microscopic process of polyethylene crystallization, the features of crystal morphology, and the influence of temperature on crystallization. Several simulations investigated the chain folded process of polyethylene.^{19,22–24} In Kavassalis' simulation of an all-trans single PE chain

with 1000 CH₂ units, the role of torsion potential in the polymer crystallization process was investigated.¹⁹ It was shown that in the presence of torsion potential the collapse process was a global process, whereas in the absence of torsion potential or at elevated temperature the locally collapsed domains were formed and subsequently coalesced to form the final collapsed state. However, Qi Liao et al.²² have pointed out that a modification of torsion potential force field adopted by Kavassalis is not essential to demonstrate the local collapse. In their simulation, the effect of chain length on the collapse mechanism of a single chain was studied. It is found that when a chain has more than 1200 CH₂ units, the relaxation proceeds via a local collapse. Comparing the result of the Langevin dynamics simulations of chains with 700 and 2000 units starting from equilibrated conformations,^{23,24} with that obtained from Kavassalis' MD simulation of a all-trans chain with 1000 units,¹⁹ we may see that the crystallization process for the chain with 700 units is more similar to the global process for the chain with 1000 CH₂ in the presence of the torsional potential, while the crystallization process for the chain with 2000 units is more similar to the local process for the chain with 1000 CH₂ in the absence of the torsional potential. To study the role of the branch in the folded process and to get a comparison with the simulation of pure polyethylene,¹⁹ we performed MD simulation of methyl branched all-trans chain with 1000 units (CH₂ + CH) along the backbone and use the same force field as in ref 19. In the simulation, though the torsional potential has been taken into account, the local collapse process can also be found, so we ascribe the local collapse mechanism of the copolymer to the nucleating seed role of the branches along the copolymer chains.²⁵

There are still other important factors (such as branch content and length) affecting the crystal properties of the copolymer, which should be investigated at the molecular level. How does the crystal property change with the increasing of the branch contents? Does side-

* Corresponding author.

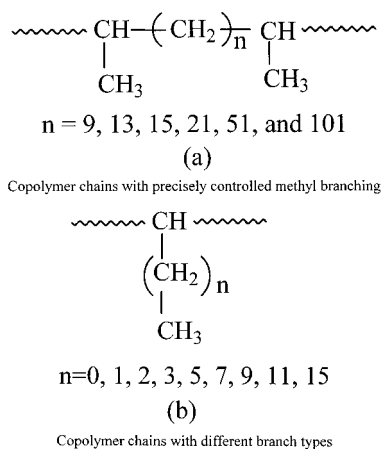


Figure 1. Schematic representation of the copolymer chain models: (a) the chains with precisely controlled methyl branching; (b) the chains with different branch types.

Table 1. Two Series of Copolymer Chain Models with Precisely Controlled Methyl Branching and with Different Branch Types

Copolymer Chains with Precisely Controlled Methyl Branching					
notation	methyl branch on every n carbon, n	total no. of CH_x units ($x = 1, 2$)	% of propene monomer (%)	simulation time (ns)	
				from extended chain	from random coil
pe-m9	9	1000	20.	4	3
pe-m13	13	1008	14.29	3	3.5
pe-m15	15	1008	12.5	3	3.5
pe-m21	21	990	9.09	2.5	4
pe-m51	51	988	3.85	1.5	4
pe-m101	101	1020	1.92	1.5	6

Copolymer Chains with Different Branch Types				
notation	branch length (no. of carbons)	no. of CH_x ($x = 1, 2$) units along the backbone	no. of α -olefin monomer	simulation
				time (ns)
pe-b1	1	201	1	1
pe-b2	2	201	1	1
pe-b3	3	201	1	1
pe-b4	4	201	1	1
pe-b6	6	201	1	1
pe-b8	8	201	1	1
pe-b10	10	201	1	1
pe-b12	12	201	1	1
pe-b16	16	201	1	1

chain crystallization take place, and in this case, what is the necessary minimum length of the side chains? In this paper, to investigate the collapse process and the lamellar structure of the copolymer with well-controlled branching as well as to make clear the questions just mentioned above, MD simulations of single copolymer chain models with precisely controlled methyl branching and with branches of different lengths are performed.

II. Model and Method

Two series of copolymer chain models with precisely controlled methyl branching and with branches of different lengths built by the Polymer Builder of Cerius² software are listed in Table 1. It should be noted that the notation of pe-mn ($n = 9, 13, 15, 21, 51, \text{ or } 101$) is used to denote the well-controlled polyethylene with methyl branches on every n carbon atom and pe-bn ($n = 1, 2, 3, 4, 6, 8, 10, 12, \text{ or } 16$) represents the polyethylene chain with one branch containing n car-

bons. The schematic representations of the polymer chains are depicted in Figure 1.

The Dreiding II force field²⁶ from Cerius² software package is used in the simulations. Following ref 19, the united atom approximation is adopted to simplify the calculations. The total potential energy E_{total} consists of four parts: (1) the bond-stretching energy E_{stretch} for two adjacent united atoms, (2) the bond-bending energy E_{bend} among three adjacent united atoms, (3) the torsion energy E_{torsion} among four adjacent united atoms, and (4) the 12-6 Lennard-Jones potential E_{vdw} between two nonbonded atoms. The total potential energy E_{total} can be expressed as

$$\begin{aligned}
 E_{\text{total}} &= E_{\text{bond}} + E_{\text{vdw}} \\
 &= E_{\text{stretch}} + E_{\text{bend}} + E_{\text{torsion}} + E_{\text{vdw}} \\
 &= \frac{1}{2}K_b(R - R_0)^2 + \frac{1}{2}K_\theta(\theta - \theta_0)^2 + \\
 &\quad \frac{1}{2}K_\phi[1 - d \cos(3\phi)] + D_0 \left[\left(\frac{\sigma}{r} \right)^{12} - 2 \left(\frac{\sigma}{r} \right)^6 \right]
 \end{aligned}$$

where R is the bond length between two adjacent atoms and R_0 the equilibrium bond length, θ the bond angle between three adjacent atoms, θ_0 the equilibrium bond angle, ϕ the dihedral angle formed by four consecutive atoms, and r the distance between two nonbonded atoms.

The canonical Nosé-Hoover molecular dynamics method is used to obtain the results on the crystallization behavior of the copolymer chains at 300 K in the simulations, where the integration time step is set to 0.001 ps and a relaxation constant for the heat bath variable is 0.1 ps. The cutoff distance for the van der Waals interaction is 10.5 Å. The duration of the simulation for each model is also listed in Table 1.

III. Results and Discussion

In this section, we will first discuss the simulation results on the crystallization behavior of the single chains with precisely controlled methyl branching starting from the extended chain and random coil conformations and, in particular, discuss the effect of the branch content on the crystallization. Then we will investigate the roles of different branch lengths in the crystallization of the copolymer.

A. Crystallization of the Chains with Precisely Controlled Methyl Branching. 1. Starting from Extended Chain Conformation. In the present simulation, we find that the collapse process of the copolymer chain with precisely methyl branching is similar to that of the random copolymer chain as discussed in ref 25. For brevity, we will not discuss this in detail. From our previous simulation of copolymer chain with 2 mol % of propene composition, it was shown that the single globule can develop to a lamellar structure.²⁵ While from the present simulation of the chain with different percents of propene, it is found that the branch content plays an important role in the determination of the single globule developing to a lamellar or not.

Figure 2 shows the morphologies of the chains with various methyl contents at the last time of each simulation. It can be easily seen that for pe-m9 an amorphous structure is formed; for pe-m13 having less methyl contents than pe-m9, some regular trans segments are formed; and for other chains with much less methyl contents, the lamellar structures are formed. With the

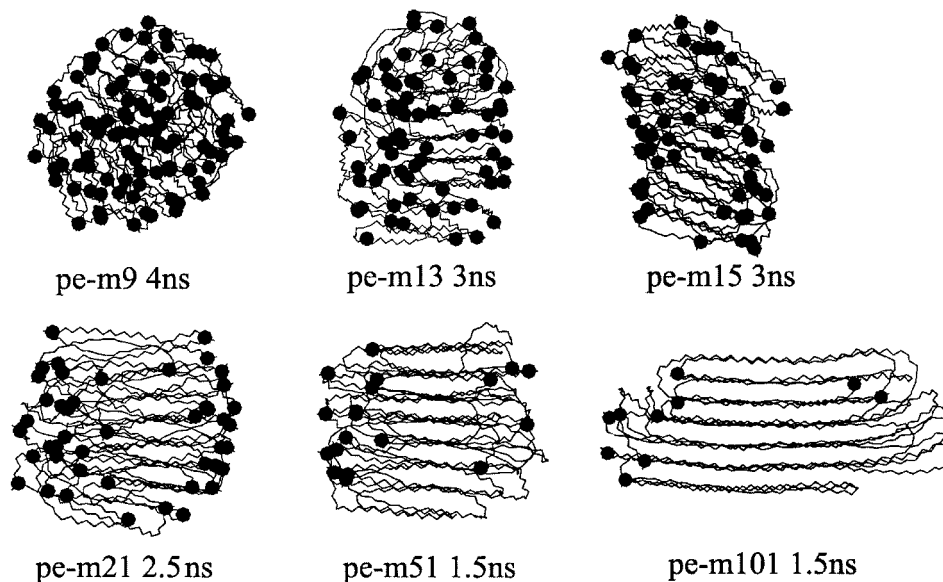


Figure 2. Morphologies of the chains with various methyl contents at the last time of each simulation, where the black balls represent the branch points.

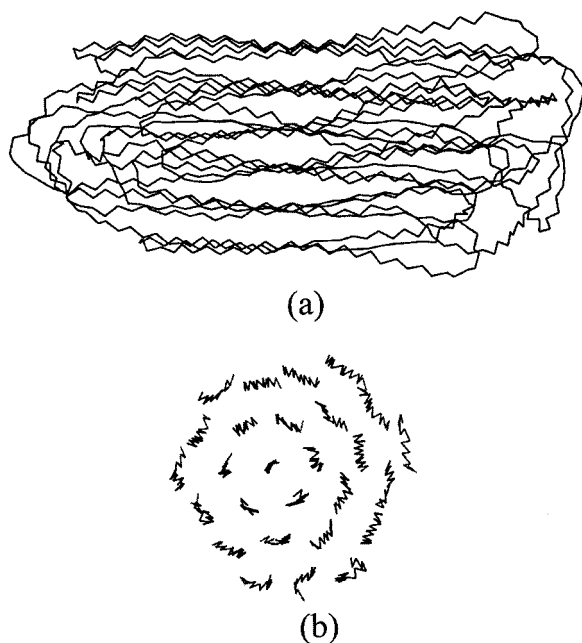


Figure 3. Lamellar structure of the PE chain at 2000 ps: (a) the side view; (b) the top view of the crystal core.

decreasing of the methyl contents, the lamellar structures become more perfect. To get a comparable result, we performed 2 ns MD simulation of a single PE chain with 1000 CH₂ units. The morphology of the PE chain at 2 ns is shown in Figure 3, where Figure 3a is the front view of the lamellar structure and Figure 3b is the top view of the crystal core of the lamella. The lamellar structure as shown in Figure 3 is similar to that obtained from Kavassalis' simulation,¹⁹ which has deformed hexagonal symmetry, and the stems in the outer layer have a tilted configuration.²⁰ From Figures 2 and 3, we can see that the lamellar structures of methyl branched chains are similar to that of the PE chain. Furthermore, from Figure 2 it is found that most of the methyl branches are located at the fold surfaces of the lamellae, which is nearly the same as in the lamellar structure obtained from the random copolymer.²⁵

It should be noted that the lamella thickness is less than 5.0 nm in the present simulation. The value is much smaller than the experimental values. This is mainly due to the small torsional barrier (2 kcal/mol) in the Dreiding II force field. Since these single-chain calculations do not account for interchain or solvent interactions, there should be some term in the potential energy function to account for these. Sundararajan attributed the smaller values of the simulated lamella dimension to the smaller torsional potential adopted in MD simulation.¹⁹ In their simulation, when the torsional barrier was increased to 6 kcal/mol, a lamella with dimension in the range of experimental values is formed.²⁷ If we use the higher torsional barrier to the simulation of the methyl branched chain, what will happen to the side groups? To make clear this, we performed 6 ns MD simulation of the pe-m51 chain with torsional barrier of 6 kcal/mol. It is found that the lamellar thickness increases to about 7.3 nm, and most of the methyl branches are still rejected to the fold surface of the lamella.

In the simulation of a single polyethylene chain with 500 CH₂ units, it was illustrated that in the bond orientationally ordered structure the gauche states were located exclusively in the fold surface (amorphous region).¹⁸ So it can be concluded that, in a lamellar structure with fixed CH₂ units, the more the trans states are contained, the better the crystallinity of the lamella is. The values of the dihedral distribution can be simply estimated by the relation $P_i = n_i / \sum n_i$, where P_i is the distribution of dihedral angle and n_i is the number of bonds in a conformation with the dihedral i ($i = -180^\circ - 180^\circ$). The dihedral distributions along the chains with various methyl branch contents are shown in Figure 4. It shows that, with the decreasing of methyl contents, the trans states increase while the gauche states decrease. This means that the crystallinity increases with the decreasing branch contents. As is well-known, the melting point and the heating of fusion of the copolymer increase with the decreasing comonomer contents.^{3,5,9,10,13} Our simulation can interpret this fact at the molecular level. As the methyl branches increase, the methylene spacing between branch points decreases (the crystallizable sequence length decreases); on the

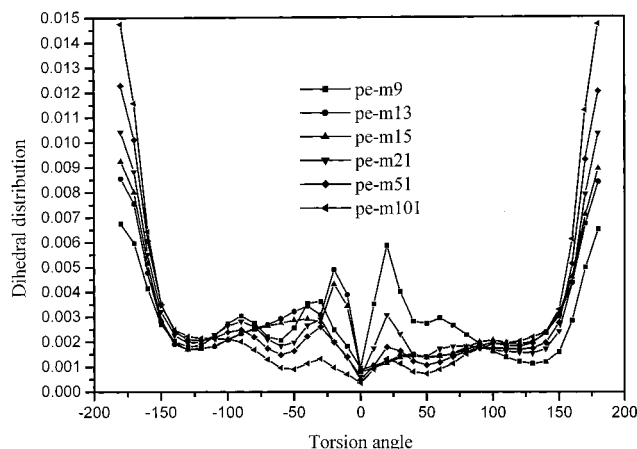


Figure 4. Dihedral distributions along the copolymer chains with different methyl branch contents.

other hand, during the formation of the lamellar structure, most of the branches are rejected to the fold surface as defects, which also results in the decreasing of the crystallizable sequence length with the increasing of the branch contents. So the crystallinity of the copolymer increases with the decreasing of the branch contents, and this leads to the increasing of the melting point and the heat fusion.

Figure 4 shows the increase in the number of trans bonds with decreasing methyl content. However, for these chains, the occurrence of near-eclipsed conformation ($\pm 20^\circ$) is more prevalent than the gauche states. It can be seen that the near-eclipsed states of various chains increase with the increasing methyl contents. On the other hand, by comparing the number of near-eclipsed conformation of the pe-51 chain obtained from the simulations using torsional barrier of 2 and 6 kcal/mol, we find that the number of near-eclipsed bonds obtained from the simulation adopting torsional barrier of 2 kcal/mol is larger. So it may be reasonable to think that there are two reasons for the occurrence of near-eclipsed conformation ($\pm 20^\circ$) being more prevalent than the gauche states: one of the reasons is the presence of methyl branches at the fold surface of the lamella; another is due to the small torsional barrier in the Dreiding force field of the Cerius² software.

Now let us discuss the variation of the potential energy and its components of the chains with different branch contents. The time averages of the potential energy and its components for each simulation starting from two configurations are listed in Table 2. It is known that in the formation process of the orientationally ordered structure E_{vdw} and $E_{torsion}$ gradually decrease.²⁰ From Table 2, it can be seen that with the decrease of branch contents E_{vdw} and $E_{torsion}$ decrease. This variation of the energy with the branch contents can also indicate

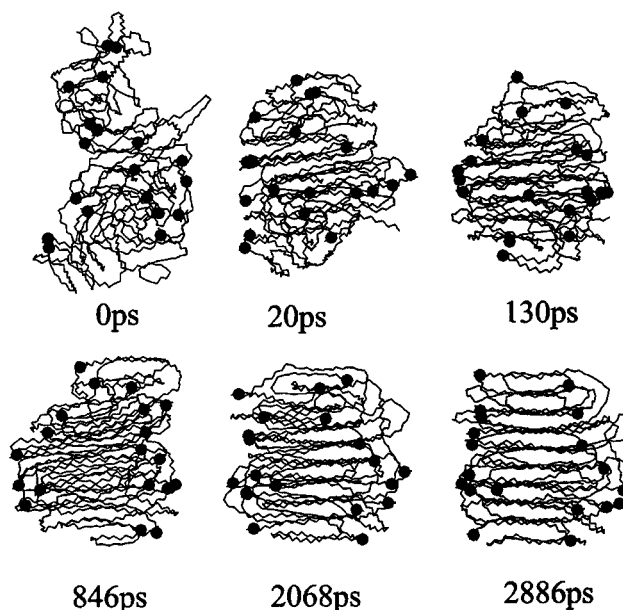


Figure 5. Collapse process of pe-m51 starting from random coil at 300 K, where the black balls represent the branch points.

that the more ordered structure formed with the branch contents decrease as mentioned above.

2. Starting from Random Coil. We have mentioned in our previous paper²⁵ that the morphology of the lamella originated from the random coil is generally similar to that from an all-trans stretched chain, which is substantiated by the similar average energies for the two starting configurations as shown in Table 2. In the present paper, for brevity, we only show the collapse process of pe-m51 starting from random coil in Figure 5. Further details of the simulation from the random coil are not presented. From Figure 5, it can be seen that the collapse process of the random coil mainly involves two stages, which is similar to the simulation results of the random copolymer starting from random coil:²⁵ First, the neighboring sequences of trans bonds aggregate together to form local ordered domains, and then they coalesce to a lamellar structure. In the process, the branches are rejected to the fold surface gradually. Since the morphology of the lamella originated from the random coil is similar to that from an all-trans stretched chain, the variations of the morphology and the crystallinity of the lamella obtained from the random coil with the branch contents have the same trends as mentioned in section III.A.1.

B. Roles of Different Branch Lengths in the Crystallization of the Copolymer. The conformations obtained from all-trans stretched chains with branches of different lengths at 1 ns are shown in Figure 6, where the big ball represents the branch point (CH unit) and

Table 2. Time Averages of the Potential Energy and Its Components for the Model Starting from Two Conformations^a

model	total potential		bond		van der Waals		torsion	
	E-t	R-c	E-t	R-c	E-t	R-c	E-t	R-c
pe-m9	-540.8	-524.61	1362.49	1360.35	-1903.29	-1884.96	611.76	607.35
pe-m13	-663.48	-667.18	1278.48	1269.42	-1941.95	-1936.60	563.15	553.67
pe-m15	-714.34	-712.74	1241.14	1239.46	-1955.48	-1952.08	535.79	536.94
pe-m21	-842.78	-878.24	1138.33	1126.5	-1981.11	-2004.74	475.56	467.84
pe-m51	-977.26	-933.65	1044.42	1060.64	-2021.68	-1994.28	427.87	440.57
pe-m101	-1144.52	-1066.06	961.25	1026.26	-2105.77	-2092.33	350.52	406.69

^a The time interval is the last 500 ps of each simulation. E-t is used to denote the extended trans conformation, and R-c denotes the random coil.

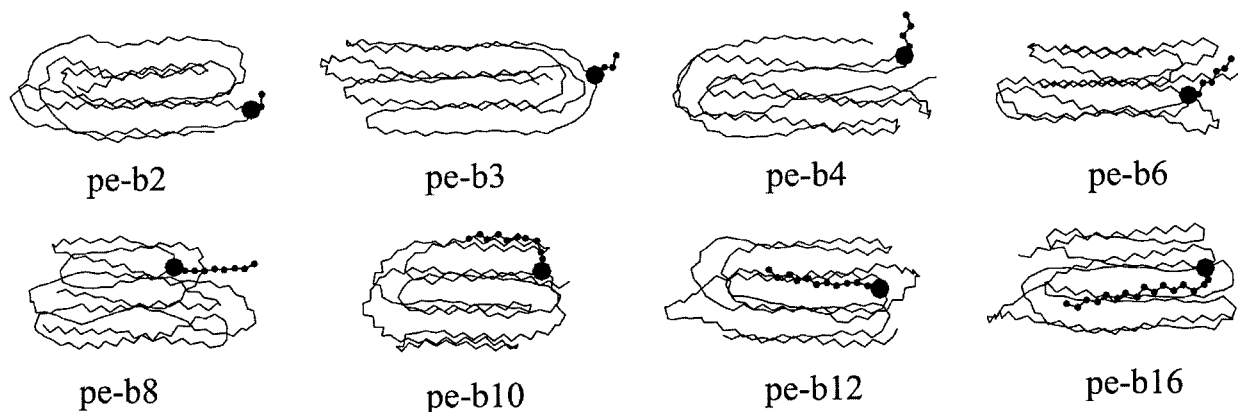


Figure 6. Conformations obtained from the all-trans stretched chains with different branch types at 1 ns, where the big ball represents the branch point and the smaller balls represent the carbons contained in the branches.

the smaller balls represent the carbons contained in the branches. It can be seen from Figure 6 that the lamellar structure is formed, and the branch point is always excluded to the fold surface for each chain, while for the branches with various lengths, different conformations are displayed. We find that when the branch chain has less than 10 carbons, the branch is expelled from the crystal region as a defect, whereas when the branch length is longer, the branch is folded back and cocrystallizes with the main chain. This indicates that the branch cannot simply be regarded as a defect point but should be considered as a defect having size effect as has been pointed out by Kim et al.³ Our simulation shows that the critical chain length for side-chain crystallization is 10 carbon atoms. Russell et al. reported experimentally that the minimum length of side chain to enter crystalline regions of ethylene-1-alkene copolymers at 298 K is probably between 10 and 12 carbon atoms,¹⁵ and in Gerum's experiment the critical length is reached in the case of hydrogenated poly[butadiene-*alt*-(1-dodecene)], which has branches with 10 carbons.⁴ Our simulation result is in harmony with the two experimental results.

As mentioned above, when the branch has more than 10 carbon atoms, the side-chain crystallization occurs. Now let us investigate the way of the side chain packed into the crystalline phase. A snapshot of the crystal core for pe-b16 at 1 ns is displayed in Figure 7, where number 6 represents the branch cocrystallizing with the main chain. It can be clearly seen that the branch and the main chain together form a lamellar structure with deformed hexagonal symmetry,^{19,20} and the distance between stems in the ordered structure ranges from 4.13 to 5.4 Å. These results are similar to the crystal structure of polyethylene in Figure 3b. This means that the side chain is packed in the same manner as in polyethylene.

The present simulation shows that the branches cocrystallize with the main chain, with their chain axis in the same direction as those of the main-chain segments in the lamella. This is with the lamella with a small dimension compared to experimental values. If we perform simulation to reproduce the experimental lamellar dimensions, will the branch still fold back, cocrystallizing with the main chain, or crystallize as a "shish-kebab" structure, sticking out of the principal lamella? The 3 ns MD simulation of the pe-b10 chain with torsional barrier of 6 kcal/mol shows that the branch still folds back and cocrystallizes with the main chain, which is shown in Figure 8. To our knowledge,

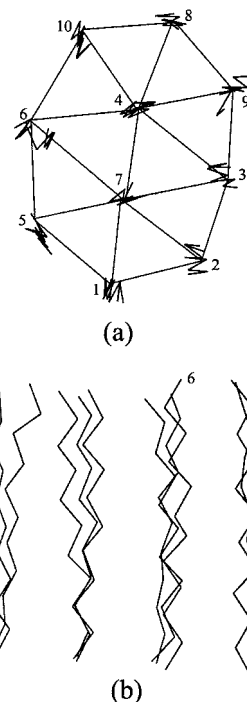


Figure 7. Snapshot of the crystal core for pe-b16 at 1 ns, where the number beside each stem denotes the stem and number 6 represent the branch cocrystallizing with the main chain.

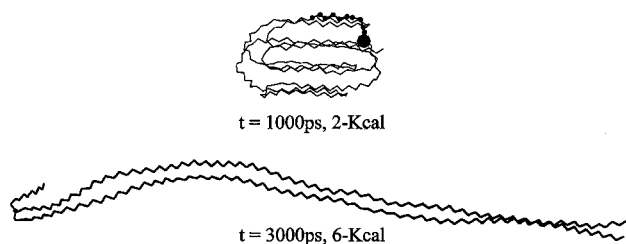


Figure 8. Morphologies of the pe-b16 chain at the last simulation time for simulation with torsional barrier of 2 and 6 kcal/mol.

there are a few experimental reports^{4,15} on the way of side chain cocrystallization with the main chain. In ref 4, though the crystal structure was not exactly determined, some data indicated a model in which the side chains were packed in a manner as in unbranched alkanes. Reference 15 reported that the crystallized side chains presented near the surface of crystallites with inner cores derived from main chains. Our simulation

result is in harmony with that of the experiments qualitatively.

IV. Conclusions

In this paper, the roles of the branch content and branch type in the copolymer crystallization are investigated by MD simulations for two series of single copolymer chain models with precisely controlled methyl branching and with branches of different lengths. From the simulations of the copolymer chains with precisely controlled methyl branching, it is found that the collapse process and the morphology of the lamellar structure are similar to those of the random copolymer. In particular, it is shown that the branch content plays an important role in determining whether a single chain can form a lamellar structure or not. With the decreasing of the branch contents, more perfect lamellar structure is formed and the crystallinity of the polymer increases. In the case of the models with branch of different lengths, it is found that the branch point is always rejected to the folded surface of the lamellar structure as a defect, while the branch should be considered as a defect having size effect. The critical chain length for side-chain crystallization is 10 carbons, and in the cocrystallization the side chain is packed in a manner as in polyethylene.

Acknowledgment. This work is supported by the Natural Science Foundation of China (G29892168, 200073014), Doctor Foundation by the Ministry of Education, Foundation for University Key Teacher by the Ministry of Education, and Key Subject of Science and Technology by the Ministry of Education of China.

References and Notes

- (1) Zhang, M.; Lynch, D. T.; Wanke, S. E. *Polymer* **2001**, *42*, 3067.
- (2) Crist, B.; Claudio, E. S. *Macromolecules* **1999**, *32*, 8945.

- (3) Kim, M.-H.; Phillips, P. J. *J. Appl. Polym. Sci.* **1998**, *70*, 1893.
- (4) Gerum, W.; Höhne, G. W. H.; Wilke, W.; Arnold, M.; Wegner, T. *Macromol. Chem. Phys.* **1995**, *196*, 3797.
- (5) Alamo, R. G.; Viers, B. D.; Mandelkern, L. *Macromolecules* **1993**, *26*, 5740.
- (6) Defoor, F.; Groeninckx, G.; Reynaers, H.; Schouterden, P.; Van der Heijden, B. *Macromolecules* **1993**, *26*, 2575.
- (7) Defoor, F.; Groeninckx, G.; Schouterden, P.; Van der Heijden, B. *Polymer* **1992**, *33*, 5186.
- (8) Wilfong, D. L. *J. Polym. Sci., Part B* **1990**, *28*, 861.
- (9) Alamo, R. G.; Mandelkern, L. *Macromolecules* **1989**, *22*, 1273.
- (10) Hosoda, S. *Polym. J.* **1988**, *20*, 383.
- (11) Clas, S. D.; Mcfaddin, D. C.; Russell, K. E.; Scammell-Bullock, M. V. *J. Polym. Sci., Part A: Polym. Chem.* **1987**, *25*, 3105.
- (12) Burfield, D. R.; Kashiwa, N. *Makromol. Chem.* **1985**, *186*, 2657.
- (13) Alamo, R.; Domszy, R.; Mandelkern, L. *J. Phys. Chem.* **1984**, *88*, 6587.
- (14) Shirayama, K.; Kita, S.-I.; Watabe, H. *Makromol. Chem.* **1972**, *151*, 97.
- (15) Russell, K. E.; Mcfaddin, D. C.; Hunter, B. K.; Heyding, R. D. *J. Polym. Sci., Part B* **1996**, *34*, 2447.
- (16) Baker, A. M. E.; Windle, A. H. *Polymer* **2001**, *42*, 681.
- (17) Smith, J. A.; Brzezinska, K. R.; Valenti, D. J.; Wagener, K. B. *Macromolecules* **2000**, *33*, 3781.
- (18) Watson, M. D.; Wagener, K. B. *Macromolecules* **2000**, *33*, 8963.
- (19) Kavassalis, T. A.; Sundararajan, P. R. *Macromolecules* **1993**, *26*, 4144.
- (20) Fujiwara, S.; Sato, T. *J. Chem. Phys.* **1997**, *107*, 613.
- (21) Fujiwara, S.; Sato, T. *J. Chem. Phys.* **2001**, *1114*, 6455.
- (22) Liao, Q.; Jin, X. *J. Chem. Phys.* **1999**, *110*, 8835.
- (23) Liu, C.; Muthukumar, M. *J. Chem. Phys.* **1998**, *109*, 2536.
- (24) Muthukumar, M.; Welch, P. *Polymer* **2000**, *41*, 8833.
- (25) Zhang, X.; Li, Z.; Lu, Z.; Sun, C. *J. Chem. Phys.* **2001**, *115*, 3916.
- (26) Mayo, S. L.; Olafson, B. D.; Goddard, W. A. III *J. Phys. Chem.* **1990**, *94*, 8897.
- (27) Sundararajan, P. R.; Kavassalis, T. A. *J. Chem. Soc., Faraday Trans.* **1995**, *16*, 2541.

MA011281D